

Network Induced Large Correlation Matrix Estimation

Shuo Chen^{1*}, Jian Kang², Yishi Xing¹, Yunpeng Zhao³, and Donald Milton⁴

¹ Department of Epidemiology and Biostatistics, University of Maryland, College Park, MD 20742, USA

² Department of biostatistics, University of Michigan, Ann Arbor, MI 48109, USA

³ Department. of Statistics, George Mason University, Fairfax, VA 22030, USA

⁴ Maryland Institute for Applied Environmental Health, University of Maryland, College Park, MD 20742, USA

Abstract

In this paper, we consider to estimate network/community induced large correlation matrices. The massive biomedical data (e.g. gene expression or neuroimaging data) often include latent networks where features are highly correlated with each other, and the correlation matrix exhibits a complex and organized, yet latent topological structure. Although current large covariance/correlation matrix and precision matrix estimating methods using thresholding or shrinkage strategies may provide satisfactory estimation of the overall matrix, they do not allow automatic network/topology detection nor integrating the topological information into correlation matrix estimation. To fill the gap, we propose a new network induced correlation estimation method (NICE) that seamlessly detects the latent and organized graph topology and then estimate the correlation matrix by leveraging an adaptive and graph topology oriented thresholding strategy. Recognizing the latent topological structure of the correlation matrix provides informative prior knowledge for the following thresholding procedure and allows edges to borrow strength from each other properly. Therefore, our graph topology oriented thresholding strategy may reduce false positive and false negative discovery rates simultaneously. Simulation results show that our approach outperforms the competing thresholding and

*Correspondence to: shuochen@umd.edu

shrinkage methods. We further illustrate the application of our new method by analyzing of a serum mass spectrometry proteomics data set.

Keywords: graph, large correlation matrix, network, shrinkage, thresholding, topology.

1 Introduction

We consider a large data set $\mathbf{X}_{n \times p}$ with the sample size n and the feature dimensionality of p . The estimation of the covariance matrix $\mathbf{\Sigma}$ or correlation matrix \mathbf{R} is fundamental to understand the inter-relationship between variables of the large data set $\mathbf{X}_{n \times p}$ (Fan *et al*, 2015).

When the dimensionality is high (p is large), the estimation by using sample covariance is known to have poor performance and regularization is needed. Various regularization methods have been developed for this purpose. For instance, ℓ_1 penalized maximum likelihood have been utilized to estimate the sparse precision matrix $\mathbf{\Theta} = \mathbf{\Sigma}^{-1}$ (Friedman *et al*, 2008; Banerjee *et al*, 2008; Yuan and Lin, 2007; Lam and Fan, 2009; Yuan, 2010; Cai and Liu, 2011; Shen *et al*, 2012). In addition, the covariance matrix thresholding methods have been developed to directly regularize the sample covariance matrix (Bickel and Levina, 08; Rothman *et al*, 2009; Cai *et al*, 2011; Zhang, 2010; Fan *et al*, 2013; Liu *et al*, 2014). Similarly, the thresholding regularization techniques have also been applied to correlation matrix \mathbf{R} estimation (Qi and Sun, 2006; Liu *et al*, 2014; Cui *et al*, 2016). Mazumder and Hastie (2012) and Witten *et al* (2011) find the two sets of methods are naturally linked regarding vertex-partition of the whole graph.

The regularization strategies including both covariance matrix thresholding and precision matrix shrinkage methods are often implemented on individual edges rather than considering the interaction between edges and the whole graph topology. Hence, a universal thresholding value or regularization standard is applied to all edges without accounting for the dependency between edges. Cai and Liu (2011) propose adaptive thresholding methods by considering the variability of the individual entries, yet such thresholding strategy still applies the same decision rule to each entry independently without accounting for the whole graph topology.

Graph theory notations and definitions are often used to delineate the relationship between the p variables of $\mathbf{X}_{n \times p}$ (Yuan and Lin, 2007; Mazumder and Hastie, 2012). A finite undirected graph $G = \{V, E\}$ consists two sets, where the vertex set V represents the variables $\mathbf{X} = (X_1, \dots, X_p)$ with $|V| = p$ and the edge set E denote relationships between the vertices. In practice, the edge set E (our main interest) is represented by a symmetric 0 and 1 adjacency matrix. Two nodes (i.e. variables) i and j are directly connected if $e_{i,j} = 1$, otherwise unconnected. Under the sparsity assumption, the regularization algorithms assign most edges as 0s, and G is decomposed to a set of maximal connected subgraphs (Witten *et al*, 2011; Mazumder and Hastie, 2012).

Previous studies show that the interactions between genes or neural processing units exhibit organized network graph topological properties (i.e. non Erdős-Rényi random graph). Recently, Cai *et al*, 2014 suggest the prior knowledge of the matrix structure may improve the regularization and estimation procedure. However, often the topological structure of covariance and precision matrices is latent and thus it is crucial to identify the topological patterns in a data-driven fashion for correlation matrix estimation. In this paper, we consider that there are latent community networks, and variables are more correlated with each other within the same community network.

The latent community graph structure is naturally linked to the stochastic block model (SBM, Bickel and Chen, 2009; Karrer and Newman, 2011; Zhao *et al*, 2011; Choi *et al*, 2012; Nadakuditi and Newman, 2012; Lei and Rinaldo, 2014). However, the high-dimensional biomedical data tend to be different from the assumption of the SBM model because not all variables can be allocated to communities. Therefore, we consider a new model structure that $G = G^1 \cup G^0$ where the subgraph $G^1 = \cup_{c=1}^C G_c$ follows a SBM and $G^0 = \cup_{m=1}^M G_m$ (G_m is a singleton only consisting one node) can be considered as a Erdős-Rényi random graph (i.e. G is a SBM-RG model). From the perspective of clustering, the SBM-RG model categorizes many nodes into communities and the rest of nodes as singletons. We develop novel algorithms to implement the automatic detection of the latent SBM-RG model from an input graph/adjacency matrix without clear patterns. The algorithms are developed in light of the ‘rule of parsimony’ which control the number and sizes of communities to ensure most variables in communities are highly correlated (i.e. ‘high quality’ communities). Our SBM-RG based community detection algorithm alone would contribute as a novel unsupervised

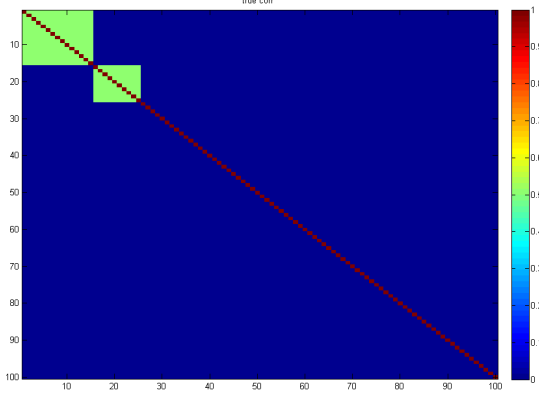
learning technique for pattern recognition.

Our overarching goal is to estimate the network induced correlation matrix by adaptive thresholding, and decision rule of thresholding is enlightened by the detected graph topological structure (i.e. the SBM-RG structure). Specifically, we perform adaptive thresholding for edges within and outside communities by using Bayes factors, and thus such differential thresholding levels are results of incorporating graph topology knowledge as priors into an universal regularization rule. In this way, the decision making of thresholding for a single edge is made upon considering both this edge’s magnitude and the edges from the same community via the detected graph topological information. and this allows us to avoid the tedious and complicated (maybe even impossible) estimation of the covariance of edges (correlation of correlations). We name this new graph topology information guided regularization strategy **Network Induced Correlation matrix Estimation (NICE)**. This strategy is distinct from the conventional graphical model based covariance/precision matrix estimation, because we first detect the non-random/organized graph topological patterns and then perform regularization by leveraging the topological patterns. We implement the NICE model in two steps and we further provide theoretical results of the proposed algorithms.

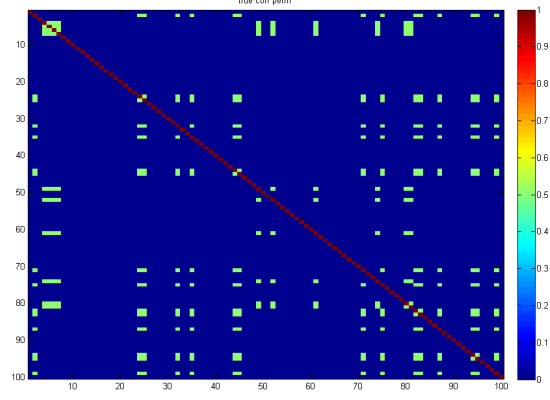
The paper is organized as follows. Section 2 describes the NICE algorithm, followed by theoretical results in Section 3. In Section 4 and 5, we perform the simulation studies and model evaluation/comparison and we apply our method to mass spectrometry proteomics data data. Concluding remarks are summarized in Section 6.

2 Methods

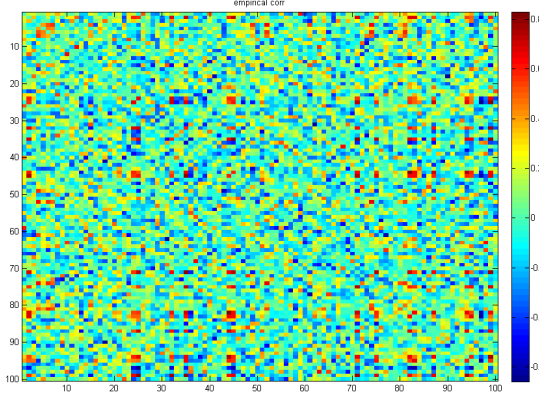
We consider the sample covariance \mathbf{S} and the correlation matrix $\hat{\mathbf{R}} = \text{diag}(\mathbf{S})^{-1/2} \mathbf{S} \text{diag}(\mathbf{S})^{-1/2}$ as our input data (Qi and Sun, 2006; Liu *et al*, 2014; Fan *et al*, 2015). We may directly perform thresholding regularization on the sample correlation matrix to estimate \mathbf{R} by using $R_{i,j}^T = \{\hat{R}_{i,j} I(|\hat{R}_{i,j}| > T)\}$, where T is a selected threshold. However, applying a universal regularization/thresholding rule (even when optimal T is provided) to each element (or column) may introduce false positives and false negatives and lead to failure to detect networks of interest. Therefore, we leverage the



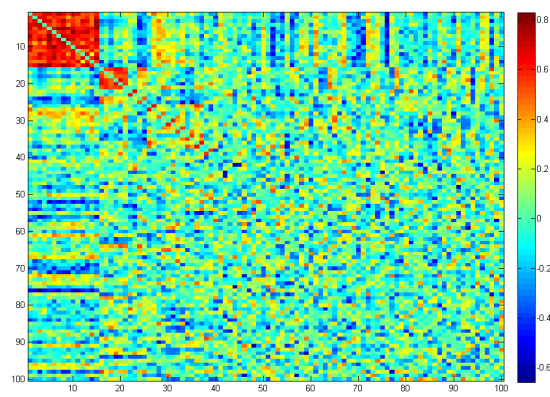
(a) The truth: two networks



(b) Shuffling the order of nodes



(c) The input data for NICE



(d) Network detection results

Figure 1: An example of a network induced covariance matrix: $|V|=100$ nodes and $|E|=4950$ edges, there are two networks (a) and in practice they are implicit (b) especially hard to recognize when looking at the sample covariance matrix (c); however, with the knowledge/estimation of topological network structures detected by NICE (d) the regularization strategy should take them into account.

automatically detected topological structure of the correlation matrix to better our decision making process.

The NICE method consists two steps: i) calculate the posterior probability weight based adjacency matrix $\mathbf{W} = g(\hat{\mathbf{R}})$ with $W_{i,j} = \text{Prob}(\delta_{i,j} = 1 | \hat{\mathbf{R}})$ as a fuzzy logic metric and then detect the SBM-RG structure $G = G^1 \cup G^0 = (\cup_{k=1}^K G_c) \cup (\cup_{m=1}^M G_m)$ by using a ‘quality and quantity rule’; ii) applying the adaptive thresholding rules to edges within and outside networks.

2.1 Graph topological structure detection

2.1.1 Calculate posterior probability based fuzzy logic weight matrix W

The adjacency matrix is crucial for topological pattern recognition. We first propose a new method to calculate the adjacency matrix from the input correlation matrix and ensure the metric of the adjacency matrix is well suited for the following topological pattern detection. Rather than directly thresholding/binarizing the sample correlation matrix $\widehat{\mathbf{R}}$ by using $\widehat{\delta}_{i,j} = I(|\widehat{R}_{i,j}| > T)$, we calculate a fuzzy logic metric $W_{i,j} = \text{Prob}(\delta_{i,j} = 1 | \widehat{\mathbf{R}})$ (Chen *et al*, 2015a). The fuzzy logic metric avoids arbitrary choice of the cut-off threshold value and provides a more appropriate scale for maximal connected component detection. Let $z_{i,j}$ be equal to the Fisher's Z transformed correlation coefficient $\widehat{R}_{i,j}$ for example (Kendall's Tau or other pairwise relationship metrics could also be applied), and $z_{i,j}$ follows two distinct distributions dependent on $\delta_{i,j}$ that $z_{i,j} | (\delta_{i,j} = 0) \sim f_0(z_{i,j})$ and $z_{i,j} | (\delta_{i,j} = 1) \sim f_1(z_{i,j})$. The f_1 represents the distribution of correlations corresponding to connected edges, and f_0 for the unconnected edges. The sample correlation coefficients follow a mixture distribution $z_{i,j} \sim \pi_0 f_0(z_{i,j}) + \pi_1 f_1(z_{i,j})$ where $\pi_0 + \pi_1 = 1$. We adopt the empirical Bayes method to obtain $\hat{\pi}_0, \hat{\pi}_1, \hat{f}_0, \hat{f}_1$, and we would refer the readers for the details to the original works (Efron, 2004; Wu *et al*, 2006; Efron, 2007). The Bayes posterior probability that a case belongs to the connected edge set given $z_{i,j}$, by definition, is:

$$\begin{aligned} E(W_{i,j}) &\equiv \text{Prob}\{\delta_{i,j} = 1 | \widehat{\mathbf{R}}\} = \pi_1 f_1(z_{i,j}) / f(z) \\ &= (f(z) - \pi_0 f_0(z_{i,j})) / f(z) \\ &= 1 - \widehat{\text{fdr}}(z_{i,j}) \end{aligned} \tag{1}$$

In practice, we calculate the fuzzy logic metric $W_{i,j} = 1 - \widehat{\text{fdr}}(z_{i,j})$ based on the estimated $\widehat{\text{fdr}}$ by using the existing statistical package e.g. 'lcfdr' in the R software.

Therefore, the Bayes posterior probability based fuzzy logic metric provides a non-parametric transformation to map the original correlation metric value of $z_{i,j}$ to a probability based 0 to 1 scale

(the probability of not be thresholded). The distribution of $W_{i,j}$ often shows a large proportion of edges with the fuzzy logic values close to zero, and a small proportion greater than zero and close to one, which clearly improves the separation of signals from noises and greatly enhances the following graph topology structure detection. Thus, this transformation could improve the performance of network structure detection. Note that \mathbf{W} is calculated as the adjacency matrix and does not involve with the regularization step.

2.1.2 Detect the SBM-RG structure by using spectral graph methods

Next, we seek to identify the SBM-RG topology of G based on the input fuzzy logic metric weight matrix \mathbf{W} . Under the assumption that the G include induced complete subgraphs (community networks) as shown in 1a, the edges within the networks are more likely to be connected than edges outside networks. However, this topological structure is latent and the sample correlation matrix has no explicit network structure (1c). Thus, our goal is to automatically recognize such graph topological structures (from 1c to 1d).

Applying a threshold to the continuous fuzzy logic metrics could not reveal the topological structure because i) the sample correlation/covariance matrix could include a large proportion of false positive and negative noises; and ii) node reordering is required to recognize the implicit pattern. For instance, applying covariance matrix thresholding rules (e.g. Bickel and Levina, 08; Friedman *et al*, 2008; and Cai and Liu, 2011) may mislead the detection of the true topological structures because such noises. Suppose G_{c1} and G_{c2} are the only two separate networks in G , and $e_{i,j} = 1|(e_{i,j} \in G_{c1} \text{ or } e_{i,j} \in G_{c2})$ and $e_{i,j} = 0$ otherwise. However, because of noises some values of $W_{i,j}$ ($i \in V_{c1}$ and $j \in V_{c2}$) could be false positively high, and hence the individual edge based decision rules would produce a few false positive result of $\hat{E}_{i,j} = 1|W_{i,j}$. Let $|V_{c1}| = |V_{c2}| = 20$ and there are 400 edges between the two networks, and we assume the false positive rate is 1% (very low), then the probability of failure to separate the two networks is equal to $1 - (1 - 0.99)^{400} = 0.982$ (assuming that the edges are independent). In addition, the other nodes (not in G_{c1} and G_{c2}) could be falsely connected to the networks G_{c1} and G_{c2} . Therefore, graph topological structure detection is formidable by using the thresholding and shrinkage strategy even if the tuning parameter (λ)

is optimal and the nodes are in the right order. One convenient pathway to reorder the nodes is to shuffle the nodes by allocating more correlated variables (nodes) to be adjacent to each other. However, the shuffling includes $p!$ options (e.g. $p! \doteq 10^{157}$ when $p = 100$) and it is impractical to exhaust all permutations. Therefore, we need algorithms to implement this goal. For example, we may identify each network by cutting edges connecting the network with the rest of the graph. Then, our goal becomes an edge cutting problem.

Spectral clustering algorithms have been applied to optimize the edge cutting problem for example using Ratio-Cut and Normalized Cut algorithms (von Luxburg, 2007; Nadakuditi and Newman, 2012). Given an appropriate number of clusters C , the spectral clustering methods provide a promising solution to cut edges and detect networks. However, different from the traditional goal of spectral clustering that allocates all nodes into C classes, we try to detect a graph G that could only include many community networks (G^1) and the rest of G can be considered as a Erdős-Rényi random graph (G^0). To detect such graph topological structure, we not only need to cut the edges between communities but also most edges in G^0 and between G^0 and G^1 because highly correlated edges in the random graph are distributed randomly (with no community structure) and thus G can be considered as a set of singletons. To cut edges of G with the above topological structure, the NormalizedCut algorithm seems not to work because it may fail to detect many of the the Erdős-Rényi random graph (von Luxburg, 2007). We propose the objective function based on the RatioCut algorithm. The edge cutting objective function is to minimize:

$$\operatorname{argmin}_{\{G_c\}_{c=1}^C} \sum_{c=1}^C \frac{\sum_{i \in G_c, j \notin G_c} W_{i,j}}{|V_c|}, \quad (2)$$

It minimizes the fuzzy logic metric values of the edges ($W_{i,j}$) between networks (including network of size one). The denominator $|V_c|$ prevents to generate with one major community and $C - 1$ singletons. Thus, the spectral clustering based decision rule is to cut those between network edges whose sum of fuzzy logic metric values is minimum. The network detection and edge cutting are obtained simultaneously when implementing minimization of 2. It is NP complex to implement the optimization of 2, and fortunately computational algorithms have been successfully developed for solutions (Shi and Malik, 2000; Chen *et al*, 2015b). It has been established (Chung, 1997) that the

1 is equivalent to

$$\operatorname{argmin} \sum_{c=1}^C \mathbf{h}_i \mathbf{L} \mathbf{h}_i = \operatorname{Tr}(\mathbf{H}' \mathbf{L} \mathbf{H}), \quad (3)$$

where $\mathbf{H}_{p \times C}$ is indicator matrix and a column h_k of \mathbf{H} is a binary $p \times 1$ vector (elements with entry value 1 indicate that they belong to the c th network). Estimating $\mathbf{H}_{p \times C}$ provides the network detection results. \mathbf{L} is the Laplacian matrix, which is defined by:

$$\mathbf{L} = \mathbf{D} - \mathbf{W}, \quad (4)$$

where $\mathbf{D} = \operatorname{diag}(\sum_j W_{i,j})$ and $i = 1, \dots, p$. We implement the optimization of **4** to estimate $\mathbf{H}_{p \times K}$ by using unnormalized spectral clustering (von Luxburg, 2007) and details are provided in the algorithm table. Furthermore, Lei and Rinaldo (2014) provides proof of consistency with regard to spectral clustering for SBM. Thus, the estimated \hat{G} is consistent to G , and when C is appropriately selected both communities and singletons can be detected. Therefore, to ensure the successful detection of the SBM-RG topological structure, we need to jointly apply the spectral clustering algorithm above and the C selection algorithm as follows.

2.1.3 C selection and regularization: the ‘quantity and quality’ criterion

It is crucial to select an appropriate number of C , because it not only influences the allocation of nodes but also the proportions of G^0 and G^1 . For example, if $C = |V|$ then all edge will be cut in G (then G is an Erdős-Rényi random graph) while if $C=1$ then no edge will be cut. Thus, it is important to select C wisely because it is the key to reveal the true graph topological structure and perform graph topology oriented regularization. Our heuristic to choose C is to maximally include informative edges ($W_{i,j}$ with larger values) into community networks (the quantity criterion) when ensuring that the detected networks has a high proportion of informative edges (the quality criterion). We consider $W_{i,j}$ with larger values as informative edges because the edges with higher

$W_{i,j}$ values are more rare and more likely for $e_{i,j}$ to be one (generally $Prob(e_{i,j} = 1) > Prob(E_{i'j'} = 1)$ if $W_{i,j} > W_{i'j'}$). Therefore, the quantity and quality criterion could help to select the C that is able to capture the graph topological structure if informative edges are non-randomly distributed. To implement the quantity and quality criterion, we define an objective function for C selection:

$$\frac{\sum_{c=1}^C \sum_{i \in G_c, j \in G_c} W_{i,j}}{\sum_{i < j} W_{i,j}} \cdot \frac{\sum_{c=1}^C \sum_{i \in G_c, j \in G_c} W_{i,j}}{\sum_{c=1}^C \sum_{i \in G_c, j \in G_c} 1}. \quad (5)$$

The first term (the proportion of informative edges included in the network with contrast to the informative edges in the whole graph) reflects the quantity criterion and the second term for the quality criterion (the proportion of informative edges in the networks with contrast to the total number of edges in those networks). The quantity criterion ensure to detect the networks when informative edges are in organized structures (power), and the quality criterion ensure the selected networks with all nodes well connected (to reduce false positive network detection). In practice, if the dimension p is massive $W_{i,j}$ could be replaced by $I(W_{i,j} > p_0)$ (e.g. $p_0 = 0.05$) to avoid the accumulation of noises (e.g. false positive errors). In addition, since we apply adaptive thresholding rules to \mathbf{W} for edges inside and outside networks, our final correlation/covariance matrix estimation is influenced by the selection of C . We implement C optimization by grid searching because C can only be integers from two to n . The NICE algorithm selects C objectively, and the overall thresholding is data-driven.

After performing the edge cutting step using spectral clustering algorithm with optimized K , we obtain the estimated clusters as $\cup_{c=1}^C \hat{G}_c = G$ (where many \hat{G}_c could be singletons). We could further examine the detected community networks with size greater than two are true networks by using permutation tests (see details in the algorithm table). The underlying heuristic is that if the detected network is a true community (organized pattern), then there are higher proportion of edges with $e_{i,j} = 1$ within the detected network and $\sum_{i,j \in G_c} W_{i,j}$ is larger than the whole graph average level.

2.2 Graph topology oriented adaptive correlation matrix thresholding

Our final goal is to threshold the correlation matrix \mathbf{R} , and we decide the threshold level based on both value of $R_{i,j}$ and the topological structure. Without loss of generality, suppose that the original universal thresholding rule (without graph topology detection) is to keep an edge when we observe the transformed correlation metric $z_{i,j}$ (e.g. Fisher's Z transformed correlation coefficient or Kendall's Tau) that

$$\frac{P(e_{i,j} = 1|z_{i,j})}{P(e_{i,j} = 0|z_{i,j})} = \frac{f_1(z)\pi_1}{f_0(z)\pi_0} \geq T, \quad (6)$$

where T is a constant, for example $T = 4$ as suggested by [Efron \(2007\)](#) which is corresponding to *locfdr* cutoff of 0.2 ([Shäfer and Strimmer, 2005](#)). If $\pi_0 = 0.9$ and $\pi_1 = 0.1$ then the universal decision rule is that $\text{BF} = \frac{f_1(z_{i,j})}{f_0(z_{i,j})} > 36$ to apply this threshold to each edge $e_{i,j}$. The detected graph topology provides additional information of the dependency structure of edges, thus the prior knowledge is updated accordingly. For network induced correlation matrix, we assume that the variables in the communities are highly correlated and thus the edges are very likely to be connected (SBM structure). The updated prior odds follow for edges within communities and outside communities:

$$\frac{P(e_{i,j} = 0|e_{i,j} \in G_c, \forall k)}{P(e_{i,j} = 1|e_{i,j} \in G_c, \forall k)} = \frac{\pi_0^{in}}{\pi_1^{in}} = \theta_{in} < 1, \text{ and } \frac{P(e_{i,j} = 0|e_{i,j} \notin G_c, \forall k)}{P(e_{i,j} = 1|e_{i,j} \notin G_c, \forall k)} = \frac{\pi_0^{out}}{\pi_1^{out}} = \theta_{out} > 1 \quad (7)$$

It has been well documented that the Bayes factor inferential models could adjust the multiplicity by adjusting the prior structure ([Jeffreys, 1961](#); [Kass and Raftery, 1995](#); [Scott and Berger, 2006](#); [Efron, 2007](#); [Scott and Berger, 2010](#)). The prior odds are tuned to control false positive rates, and a larger π_0 (or a distribution of π_0 , and larger means $\pi_0 \rightarrow 1$) leads to more stringent adjustment that may cause both low false positive discovery rates and high false negative discovery rates. [Scott and Berger, 2006](#) suggest a prior distribution with median value around 0.9 and [Efron, 2007](#) estimates π_0 by using a empirical Bayes model. These tuning methods are developed for the node based (e.g. gene expression or brain activation analysis) inference, and the correlation matrix thresholding requires

edge level inference. Since edges are dependent with each other, the mass univariate inference ignoring the dependency may lead to poor false positive and negative rates, whereas the estimation of the dependency structure between edges could be challenging. Therefore, we leverage the prior knowledge of topological structure for adaptive thresholding which is equivalent to adjusting the dependency structure.

In step two, we have identified the latent communities where variables are highly correlated. The graph topology (SBM-RG structure) oriented adaptive thresholding rule is:

If $e_{i,j} \in G_c$,

$$\hat{\rho}_{i,j} = \begin{cases} R_{i,j} & \text{if } BF_{i,j} = \frac{\hat{f}_1(z_{i,j})}{\hat{f}_0(z_{i,j})} \geq T \cdot \hat{\theta}_{in}; \\ 0 & \text{otherwise.} \end{cases}$$

else if $e_{i,j} \notin G_c$,

$$\hat{\rho}_{i,j} = \begin{cases} R_{i,j} & \text{if } BF_{i,j} = \frac{\hat{f}_1(z_{i,j})}{\hat{f}_0(z_{i,j})} \geq T \cdot \hat{\theta}_{out}; \\ 0 & \text{otherwise.} \end{cases}$$

The above decision rule is simply a fusion of graph topology oriented priors and the universal Bayes factor. Therefore, our adaptive thresholding rule relies on the community structure and we have a belief that edges within a community are more likely to be truly connected. A community is similar to a neighborhood (spatial closeness) with explicit boundaries and the elements within the neighborhood could borrow power from each other. Many statistical models are developed based on this idea, for example, the Ising prior and conditional autoregressive (CAR) model ([Besag and Kooperberg, 1995](#)). Nevertheless, unlike spatial or imaging statistics the correlation/covariance matrix of large biomedical data sets often include no available information about spatial location or closeness. The community/network detection algorithm in section 2.2 provides a pathway to learn this latent information. Furthermore, since each community has a clear boundary, edges can not only borrow strength from each other within one community but also acquire prior information of the distribution of all edges within a community (i.e. $\hat{\theta}_{in}$). Therefore, our adaptive rule could account for the dependency between edges.

In practice, $\hat{\theta}_{in}$ and $\hat{\theta}_{out}$ could be directly estimated from the data. First, all edges in \mathbf{R} (Fisher's Z transformed correlation coefficients) follow a mixture distribution $f(z_{i,j}) = \pi_0 f_0(z_{i,j}) + \pi_1 f_1(z_{i,j})$, and $\hat{\pi}_0, \hat{\pi}_1, \hat{f}_0, \hat{f}_1$ are estimated in Step 1. Next, we let all edges $z_{i,j}$ that $e_{i,j} \in G_c$ within detected communities follow a distribution $f^{in}(z_{i,j}) = \pi_0^{in} f_0(z_{i,j}) + \pi_1^{in} f_1(z_{i,j})$, and we only need to estimate $\hat{\pi}_0^{in}$ by maximum likelihood estimation (MLE) using \hat{f}_0, \hat{f}_1 estimated in the previous step. $\hat{\theta}_{in} = \hat{\pi}_1^{in} / \hat{\pi}_0^{in}$. Similarly, we let edges outside of network ($z_{i,j}$ that $e_{i,j} \notin G_c$) $f^{out}(z_{i,j}) = \pi_0^{out} f_0(z_{i,j}) + \pi_1^{out} f_1(z_{i,j})$ and estimate $\hat{\pi}_0^{out}$ by MLE and estimated \hat{f}_0, \hat{f}_1 . In general, $f = f^{in} + f^{out}$. In practice, the prior odds ratio θ_{in}/θ_{out} is larger if the (correlation coefficient) distributions of within and outside community edges are farther apart.

Remarks: the statistical inferences on large covariance/correlation matrices involve multiple aspects such as topological structures and covariance matrix estimation. It is limited to simply apply a one (or two) step of universal decision rule for knowledge/data mining. Recognizing the graph topological structure provides a fundamental understanding of the interactive relationships between multivariate variables. In turns, the topological structure could become prior knowledge to improve topological structure assisted large covariance/correlation matrix regularization and estimation. We summarize the NICE algorithm of all two steps in Algorithm 1.

Algorithm 1 NICE algorithm

- 1: **procedure** NICE–ALGORITHM
 - 2: Obtain the empirical Bayes fuzzy logic matrix $\mathbf{W} = g(\mathbf{R})$
 - 3: Calculate the Laplacian matrix $L = D - \mathbf{W}$
 - 4: **for** cluster number $K = 2 : |V| - 1$ **do**
 - 5: Compute the first K eigenvectors $[u_1, \dots, u_K]$ of L , with eigenvalues ranked from the smallest.
 - 6: Let $U = [u_1^T, \dots, u_K^T]$ be a $|V| \times K$ matrix containing all K eigenvectors.
 - 7: Perform K-means clustering algorithm on U with K to cluster $|V|$ nodes into K networks
 - 8: Calculate the quality and quantity criterion for each K .
 - 9: **end for**
 - 10: Adopt the clustering results using the K of the maximum score of the quality and quantity criterion.
 - 11: Identify the networks with significantly high proportion of larger fuzzy logic values by permutation test: for each network in \mathbf{W}
 - i) calculate the $T_k^0 = \sqrt{\sum_{i,j \in G_c} -\log(W_{i,j}) / (|E_k|)}$;
 - ii) list all $\{W_{i,j}\}$ in \mathbf{W} as a vector and shuffle the order of the vector and assemble the shuffled vector as a permuted \mathbf{W}^m for M (e.g. 10,000) times;
 - iii) calculate the maximum statistic T_{max}^m for all detected communities in each iteration;
 - iv) calculate the percentile of T_k^0 in $\{T_{max}^m\}$, if it is less than the α level then the network k is considered as a true community network.
 - 12: Implement the topological structure oriented thresholding strategies for covariance entries inside and outside networks (see details in 2.3)
 - 13: **end procedure**
-

3 Theoretical Results

We start with some notations. Let $X_{i,k}$ be the observed data on node i for subject k , for $i = 1, \dots, p_n$ and $k = 1, \dots, n$. Let $\mathbf{R} = \{\rho_{i,j}\}$ be the true correlation matrix of interests with $\text{Cor}(X_{i,k}, X_{j,k}) = \rho_{i,j}$ and $\hat{\mathbf{R}} = \{\hat{\rho}_{i,j}^{(n)}\}$ be the correlation matrix estimator. Let $\text{Fis}(x) = \log \{(1+x)/(1-x)\}/2$ be the Fisher's Z transformation. Let $z_{i,j}^{(n)} = \text{Fis}(\hat{\rho}_{i,j}^{(n)})$ and $\mu_{i,j} = \text{Fis}(\rho_{i,j})$. Note that we have $\rho_{i,j} = 0$ if and only if $\mu_{i,j} = 0$. Let $f_{i,j}^{(n)}(\cdot)$ be the density function of $z_{i,j}^{(n)}$. Let $\phi(x) = \exp(-x^2/2)/\sqrt{2\pi}$ be the standard normal density function. Let $e_{i,j} = I[\rho_{i,j} \neq 0] = I[\mu_{i,j} \neq 0]$.

Let $q_n = \sum_{1 \leq i < j \leq p_n} e_{i,j}$,

$$f_0^{(n)}(z) = \frac{\sum_{i < j} (1 - e_{i,j}) f_{i,j}^{(n)}(z)}{\sum_{i < j} (1 - e_{i,j})}, \quad \text{and} \quad f_1^{(n)}(z) = \frac{\sum_{i < j} e_{i,j} f_{i,j}^{(n)}(z)}{\sum_{i < j} e_{i,j}}.$$

Let $f^{(n)}(z)$ denote the actual distribution of $\{z_{i,j}^{(n)}\}_{1 \leq i < j \leq p_n}$.

$$f^{(n)}(z) = \pi_0^{(n)} f_0^{(n)}(z) + \pi_1^{(n)} f_1^{(n)}(z),$$

where

$$\pi_0^{(n)} = \frac{p_n(p_n - 1) - q_n}{p_n(p_n - 1)} \quad \text{and} \quad \pi_1^{(n)} = 1 - \pi_0^{(n)}.$$

Given data $\{z_{i,j}^{(n)}\}_{i < j}$, suppose $\hat{f}_k^{(n)}(\cdot)$ be an estimator for $f_k^{(n)}(\cdot)$ for $k = 0, 1$, and $\hat{\pi}_0^{(n)}$ is an estimator for $\pi_0^{(n)}$ with $\hat{\pi}_1^{(n)} = 1 - \hat{\pi}_0^{(n)}$. For any $T > 0$ and $\hat{\mathbf{R}}$, define the adaptive thresholding operator $A(\hat{\mathbf{R}}; T) = \{A(\hat{\rho}_{i,j}^{(n)}; T)\}_{i < j}$. Specifically,

$$A(\hat{\rho}_{i,j}^{(n)}; T) = \begin{cases} \hat{\rho}_{i,j}^{(n)}, & \frac{\hat{f}_1^{(n)}(z_{i,j}^{(n)})}{\hat{f}_0^{(n)}(z_{i,j}^{(n)})} > \frac{\hat{\pi}_0^{(n)}}{\hat{\pi}_1^{(n)}} T, \\ 0 & \frac{\hat{f}_1^{(n)}(z_{i,j}^{(n)})}{\hat{f}_0^{(n)}(z_{i,j}^{(n)})} \leq \frac{\hat{\pi}_0^{(n)}}{\hat{\pi}_1^{(n)}} T. \end{cases}$$

3.1 Conditions

The following conditions are needed to facilitate the technical details, although they may not be the weakest conditions.

Condition 3.1. *We consider the following conditions on the data $\mathbf{X} = (X_{i,k})$.*

1. *Data are centered around zero with unit variance. i.e $E[X_{i,k}] = 0$ and $\text{Var}[X_{i,k}] = 1$.*

2. *Data are uniformly bounded. That is, there exists a constant $M > 0$ such that*

$$\Pr[|X_{i,k}| < M] = 1,$$

3. *The Pearson's correlation estimator is computed by*

$$\hat{\rho}_{i,j}^{(n)} = \frac{1}{n} \sum_{k=1}^n X_{i,k} X_{j,k},$$

4. *The population level correlation satisfy*

$$|\rho_{i,j}| = |E[X_{i,k} X_{j,k}]| < 1.$$

for all $1 \leq i, j \leq p_n$ and $k = 1, \dots, n$.

Condition 3.2. *There exist constants $c_0 > 0$ and $\tau > 0$, such that*

$$\mu_{\inf} = \inf_{i < j} \{|\mu_{i,j}| : e_{i,j} = 1\} = c_0 n^{-1/2+\tau}.$$

Condition 3.3. *Let $\tau > 0$ be the same constant in Condition 3.2. Then*

$$\log(p_n) = o(n^{2\tau}).$$

Condition 3.4. *Suppose there exists $0.5 < \pi_0 < 1$, such that*

$$\lim_{n \rightarrow \infty} \pi_0^{(n)} = \pi_0 \text{ and } \lim_{n \rightarrow \infty} \pi_1^{(n)} = 1 - \pi_0.$$

Condition 3.5. *Given data $\{z_{i,j}^{(n)}\}_{i < j}$, suppose $\hat{f}_k^{(n)}(\cdot)$ be a consistent estimate for $f_k^{(n)}(\cdot)$ for $k =$*

0, 1. Suppose $\widehat{\pi}_0^{(n)}$ is consistent estimates for $\pi_0^{(n)}$. Specifically, for any $\epsilon > 0$,

$$\lim_{p_n \rightarrow \infty} \Pr\{\|\widehat{f}_k^{(n)}(\cdot) - f_k^{(n)}(\cdot)\|_2 + |\widehat{\pi}_0 - \pi_0| > \epsilon\} = 0.$$

where $\|\cdot\|_2$ be the L_2 norm for the function, which is defined as $\|f\|_2 = \int_{\mathbb{R}} \{f(x)\}^2 dx$.

3.2 Tail Probability Bounds

By Berry-Esseen theorem and Taylor expansion, it is straightforward to show the following lemma:

LEMMA 3.1. For any $i < j$,

$$\lim_{n \rightarrow \infty} \sup_{z \in \mathbb{R}} \left| f_{i,j}^{(n)}(z) - \sqrt{n} \phi\{\sqrt{n}(z - \mu_{i,j})\} \right| = 0.$$

In addition, we also need to study the probability bound of the $z_{i,j}^{(n)}$. Specifically, we have the following lemma:

LEMMA 3.2. Suppose Condition 3.1 holds. For all $1 \leq i, j \leq p_n$, there exists a constant $K > 0$ and $N > 0$, for and $n > N$, and any $\epsilon > 0$, we have

$$\Pr[\sqrt{n}|z_{i,j}^{(n)} - \mathbb{E}[z_{i,j}^{(n)}]| > \epsilon] \leq \exp(-K\epsilon^2).$$

By Lemma 3.1 and Condition 3.1, we can uniformly approximate $f_1^{(n)}(z)/f_0^{(n)}(z)$, which is stated in the following lemma:

LEMMA 3.3.

$$\begin{aligned} \lim_{n \rightarrow \infty} \sup_{z \in \mathbb{R}} \left| f_0^{(n)}(z) - \sqrt{n} \phi\{\sqrt{n}z\} \right| &= 0, \\ \lim_{n \rightarrow \infty} \sup_{z \in \mathbb{R}} \left| f_1^{(n)}(z) - \frac{1}{q_n} \sum_{i < j} e_{i,j} \sqrt{n} \phi\{\sqrt{n}(z - \mu_{i,j})\} \right| &= 0, \end{aligned}$$

and

$$\lim_{n \rightarrow \infty} \sup_{z \in \mathbb{R}} \left| \frac{f_1^{(n)}(z)}{f_0^{(n)}(z)} - \frac{\pi_0^{(n)}}{\pi_1^{(n)}} \frac{\sum_{i < j} e_{i,j} \phi\{\sqrt{n}(z - \mu_{i,j})\}}{(p_n(p_n - 1)/2 - q_n) \phi(\sqrt{n}z)} \right| = 0,$$

LEMMA 3.4. Suppose Conditions 3.2–3.4 hold. There exist constants $C_0 > 0$ and $C_1 > 0$ such that for any $i < j$ and any $T > (1 - \pi_0)/\pi_0$, there exists $N_T > 0$, for all $n > N_T$, we have when $e_{i,j} = 1$, then

$$\Pr \left[\frac{\sum_{i' < j'} e_{i',j'} \phi\{\sqrt{n}(z_{i,j}^{(n)} - \mu_{i',j'})\}}{\{p_n(p_n - 1)/2 - q_n\} \phi(\sqrt{n}z_{i,j}^{(n)})} \leq T \right] \leq \exp(-C_1 n^{2\tau}).$$

And when $e_{i,j} = 0$, then

$$\Pr \left[\frac{\sum_{i',j'} e_{i',j'} \phi\{\sqrt{n}(z_{i,j}^{(n)} - \mu_{i',j'})\}}{\{p_n(p_n - 1)/2 - q_n\} \phi(\sqrt{n}z_{i,j}^{(n)})} > T \right] \leq C_2 \exp(-C_0 n^{2\tau}).$$

Note that N_T depends on T but it does not depend on i and j .

3.3 Selection and Estimation Consistency

We construct the population level selection indicator $e_{i,j}^{(n)}(T)$ and the selection indicator estimator $\hat{e}_{i,j}^{(n)}(T)$ and discuss their properties in Lemmas 3.5 and 3.6 respectively.

LEMMA 3.5. Suppose Conditions 3.2–3.4 hold. For all $i < j$ and any $T > (1 - \pi_0)/\pi_0$, let

$$e_{i,j}^{(n)}(T) = I \left[\frac{\pi_1^{(n)} f_1^{(n)}(z_{i,j}^{(n)})}{\pi_0^{(n)} f_0^{(n)}(z_{i,j}^{(n)})} > T \right].$$

Then there exist $N_T > 0$, $C_3 > 0$ and $C_4 > 0$ such that for any $n > N_T$,

$$\Pr\{e_{i,j}^{(n)}(T) \neq e_{i,j}\} \leq C_3 \exp(-C_4 n^{2\tau}).$$

where N_T depends on T but not on i and j , and $\tau > 0$ is the same constant in Condition 3.2.

LEMMA 3.6. For any $T > (1 - \pi_0)/\pi_0$ and any $i < j$, let

$$\widehat{e}_{i,j}^{(n)}(T) = I \left[\frac{\widehat{\pi}_1^{(n)} \widehat{f}_1^{(n)}(z_{i,j}^{(n)})}{\widehat{\pi}_0^{(n)} \widehat{f}_0^{(n)}(z_{i,j}^{(n)})} > T \right].$$

Then there exists $N_T > 0$ such that for all $n > N_T$,

$$\Pr[\widehat{e}_{i,j}^{(n)}(T) \neq e_{i,j}] \leq C_3 \exp(-C_4 n^{2\tau}),$$

where the constants C_3 , C_4 and τ are the same as the ones in Lemma 3.5.

We establish the selection consistency and estimation consistency in the following two theorems respectively.

THEOREM 1. (Selection Consistency) Suppose Conditions 3.1 – 3.5 hold. Denote by $\mathbf{E} = \{e_{i,j}\}_{i < j}$ all the edge indicators. For any $T > (1 - \pi_0)/\pi_0$, let $\widehat{\mathbf{E}}(T) = \{\widehat{e}_{i,j}^{(n)}(T)\}_{i < j}$, then there exists $N_T > 0$ for all $n > N_T$,

$$\Pr\{\widehat{\mathbf{E}}(T) = \mathbf{E}\} \geq 1 - \frac{C_3}{2} p_n(p_n - 1) \exp(-C_4 n^{2\tau}).$$

where the constants C_3 , C_4 and τ are the same as the ones in Lemma 3.5. Furthermore,

$$\lim_{n \rightarrow \infty} \Pr\{\widehat{\mathbf{E}}(T) = \mathbf{E}\} = 1.$$

THEOREM 2. (Estimation Consistency) Suppose Conditions 3.1 – 3.5 hold and the constant τ in Condition 3.5 satisfies $0 < \tau < 1/2$. For any $\epsilon > 0$ and any $T > (1 - \pi_0)/\pi_0$, we have

$$\lim_{n \rightarrow \infty} \Pr[\|A(\widehat{\mathbf{R}}; T) - \mathbf{R}\|_\infty > \epsilon] = 0,$$

where $\|\mathbf{M}\|_\infty$ is the L^∞ norm, i.e. $\|\mathbf{M}\|_\infty = \max_{1 \leq i, j \leq p_n} |m_{i,j}|$ for any matrix $\mathbf{M} = (m_{i,j})$.

4 Simulation Studies

We conduct numerical studies to evaluate the performance of NICE algorithm for detecting the correlated networks and estimating covariance matrix, and compare it with the other popular large covariance matrix shrinkage and thresholding method.

4.1 Simuluation datasets

We simulate a data set with $p = 100$ variables, and thus $|V| = 100$ and $|E| = \binom{100}{2} = 4950$. We assume that the covriance matrix includes two induced correlated networks, and the first include 15 nodes and the second 10 nodes. The induced networks are complete subgraphs that all edges are connected within these two networks and no other edges are connected outside the two networks (Fig 1a). Next, we permute the order of the nodes to mimic the practical data sets that the network structures are implicit (Fig 1b), which represents the true edge set E . Let X_p follow a multivariate normal distribution, with zero mean and covariance matrix $\Sigma_{p \times p}$, and the sample size is N . $\sigma_{i,j}$ is an entry at the i th row and j th column of Σ , $\sigma_{i,j} = 1$ if $i = j$, and $\sigma_{i,j} = \rho|e_{i,j} = 1$ for edges within the networks and $\sigma_{i,j} = 0|e_{i,j} = 0$ for edges outside the networks. We simulate 100 data sets at different signal to noise (SNR) levels by using sample sizes N and different values of ρ (Fig 1c) as a) a larger sample size reduces the asymptotic variance of $\hat{\sigma}_{i,j}$ and thus the noise level is lower (for larger N); b) a higher absolute value of ρ represents higher signal level. We compare our method with glasso, CLIME, and adaptive thresholding by comparing the false positive and negative rates of $\hat{E}_{i,j}$ with contrast to the ground truth regarding the network detection and edge set E estimation. We assess the performance of each method by estimating the number of false positive (FP) edges $\hat{e}_{i,j} = 1|e_{i,j} = 0$ and false negative (FN) edges $\hat{e}_{i,j} = 0|e_{i,j} = 1$. In our simulated data sets, 150 edges are connected $e_{i,j} = 1$ and 4800 edges are unconnected $e_{i,j} = 0$. For inverse covariance matrix shrinkage and covariance matrix thresholding methods we treat the the non-zero entry as $\hat{e}_{i,j} = 1$ and then summarize the FP and FN edges because they provide the same estimate of E (Mazumder and Hastie, 2012).

Table 1: Median and quantiles of FP and FN

Parameters	$\sigma = 0.5$	$sample\ size = 25$	$\sigma = 0.5$	$sample\ size = 50$	$\sigma = 0.7$	$sample\ size = 25$
	FP	FN	FP	FN	FP	FN
<i>glasso</i> _{0,1}	1673(1648,1702)	59(55,64)	1621(1591.5,1640)	44(40,46)	1581.5(1557,1606)	45.5(42,48)
<i>glasso</i> _{0,2}	1008.5(989,1025)	59(53.5,64.5)	630(610,644)	38(33.5,43)	932.5(920,955.5)	36(32,40)
<i>glasso</i> _{0,3}	546(529.5,560)	56(48,63.5)	151(141,162.5)	38(30.5,43)	500.5(490,516)	28(23.5,33)
<i>glasso</i> _{0,4}	211.5(200.5,222.5)	60(50.5,72)	19(16,21)	48.5(38,58)	194(186,204.5)	24.5(20,29)
<i>glasso</i> _{0,5}	51(46,59)	80.5(66,96)	1(0,2)	82.5(67,96.5)	47(41.5,54)	28(22.5,35)
<i>glasso</i> _{0,6}	7(5,10)	112.5(97,125.5)	0(0,0)	130(118.5,137)	6(5,8.5)	41(31,51)
<i>glasso</i> _{0,7}	0(0,1)	140(131.5,146)	0(0,0)	149(147,150)	0(0,1)	75(61.5,89)
<i>glasso</i> _{0,8}	0(0,0)	149(148,150)	0(0,0)	150(150,150)	0(0,0)	127(119.5,135)
<i>glasso</i> _{0,9}	0(0,0)	150(150,150)	0(0,0)	150(150,150)	0(0,0)	149(149,150)
<i>glasso</i> ₁	0(0,0)	150(150,150)	0(0,0)	150(150,150)	0(0,0)	150(150,150)
<i>CLIME</i> _{0,1}	1082.5(1047.5,1108)	56(48,64.5)	993.5(981,1024)	39(32,45.5)	1054(1021,1079)	48.5(40,56)
<i>CLIME</i> _{0,2}	353(339.5,367.5)	79.5(69,87.5)	241.5(231.5,251.5)	61(54,67.5)	345(328,359)	70(59,78)
<i>CLIME</i> _{0,3}	63(57,69)	110(98.5,115)	25(22,29)	92(84.5,100)	64(59,68)	98(87,103)
<i>CLIME</i> _{0,4}	0(0,1)	140(135,144)	0(0,0)	130(124,135)	0(0,1)	134(129,139)
<i>CLIME</i> _{0,5}	0(0,0)	150(150,150)	0(0,0)	150(150,150)	0(0,0)	150(150,150)
<i>Thres</i> _{0,1}	2017.5(1963.5,2067.5)	0(0,2)	1978.5(1944.5,2021.5)	0(0,0)	2021.5(1968.5,2061)	0(0,1)
<i>Thres</i> _{0,3}	1292.50(1252,1331)	2(0,5)	1249.5(1220.5,1288.5)	0(0,0)	1293.5(1251,1341.5)	1(0,3)
<i>Thres</i> _{0,5}	721.5(699,752)	5(1,12)	689(673.5,721)	0(0,1)	722(693,756)	3(1,10.5)
<i>Thres</i> _{0,7}	344.5(325,360)	14(7,26.5)	328.5(311.5,349.5)	1(0,2)	342.5(324,363)	10(3,21.5)
<i>Thres</i> _{0,9}	132(121,143.5)	30(18,45)	129.5(121,142)	3(1,7)	133(123.5,146)	24(12,39.5)
<i>Thres</i> _{1,1}	41.5(35,46)	55.5(40,78.5)	40.5(36.5,47.5)	10(4.5,17)	40(35.5,46.5)	49.5(28,63)
<i>Thres</i> _{1,3}	9(6,10)	92(74,112)	10(8,12)	25(13,37)	9(6,11)	78(54.5,89)
<i>Thres</i> _{1,5}	1(0,2)	126(112.5,137)	2(1,3)	50.5(32.5,68)	1(0,2)	106(92.5,114)
<i>Thres</i> _{1,7}	0(0,0)	145(138.5,148)	0(0,0)	85.5(67,102.5)	0(0,0)	132.5(120.5,138.5)
<i>Thres</i> _{1,9}	0(0,0)	150(149,150)	0(0,0)	120.5(105,130)	0(0,0)	147(144,149)
<i>AThres</i> _{0,3}	2593(2566.5,2627.5)	2(0,5)	2538.5(2509.5,2571)	0(0,0)	2594(2563,2619)	1(0,3)
<i>AThres</i> _{0,5}	1460(1421.5,1486)	5(1,12)	1412.5(1379.5,1440)	0(0,1)	1453(1419.5,1491)	3(1,10.5)
<i>AThres</i> _{0,7}	691.5(667,717)	14(7,26.5)	668.5(646,697)	1(0,2)	695.5(665.5,720)	10(3,21.5)
<i>AThres</i> _{0,9}	271.5(258,291.5)	30(18,45)	265(252,283.5)	3(1,7)	270.5(255.5,288)	24(12,39.5)
<i>AThres</i> _{1,1}	83(75,95)	55.5(40,78.5)	85(75.5,95.5)	10(4.5,17)	82(74,89.5)	49.5(28,63)
<i>AThres</i> _{1,3}	18(15,21)	92(74,112)	22(18.5,25.5)	25(13,37)	18(14.5,22)	78(54.5,89)
<i>AThres</i> _{1,5}	2(1,4)	126(112.5,137)	4(3,6)	50.5(32.5,68)	3(1,3)	106(92.5,114)
<i>AThres</i> _{1,7}	0(0,0)	145(138.5,148)	0(0,1)	85.5(67,102.5)	0(0,0)	132.5(120.5,138.5)
<i>AThres</i> _{1,9}	0(0,1)	150(149,150)	0(0,0)	120.5(105,130)	0(0,0)	147(144,149)
<i>NICE</i>	44(15,98)	3(0,27)	11(1,30)	0(0,4)	32.5(13.5,71)	14(4,38.5)

4.2 Numerical Results

The simulation results are summarized in Table 1. Rather than selecting a single tuning parameter λ for glasso by cross-validation, we explore all possible choices in the reasonable range. We utilize 25%, 50%, and 75% of the FP and FN edges of the 100 simulation data sets to evaluate the performance of the methods. The results show the NICE algorithm outperform the other methods even when comparing with the optimal tuning parameters. One possible reason could be the NICE algorithm thresholds the covariance matrix based on the topological structure rather than the a universal shrinkage or thresholding strategy. More importantly, our NICE method is the only method can automatically detect the underlying network structures. The matrix norm loss is not compared, because the networks are small and norm comparison only reflects the false positives of the outside network components. Thus, the numerical results demonstrate that our new method not only provides more accurate estimation of the covariance matrix and the edge set E than the competing method, but also automatically detects the networks where high connectivity edges distribute in an organized fashion.

5 Data example

We further apply our method to a publicly available mass spectrometry proteomics data set (Yildiz *et al*, 2007). The study collected matrix-assisted laser desorption ionization mass spectrometry (MALDI MS) data sets to obtain the most abundant peptides in the serum that may distinguish lung cancer cases from matched controls. The study included 182 subjects in the training data set and 106 in the testing data set. The raw data were 288 mass spectra for all subjects, and each raw spectrum consists roughly 70,000 data points. After preprocessing steps including MS registration, wavelets denoising, alignment, peak detection, quantification, and normalization (Chen *et al*, 2009), 184 features are considered to represent the most abundant protein and peptide features in the serum. Each feature is located at a distinct m/z value that could be linked to a specific peptide or protein with some ion charges (feature id label). The original paper intended to utilize the proteomics data to enhance disease diagnosis and prediction. In this paper, we estimate the

covariance/correlation matrix to investigate the relationship between these features. We use the training data set to calculate the sample correlation matrix as our input data $\mathbf{X}_{n \times p}$.

Next, we apply our NICE method to estimate the covariance matrix and to detect the correlated peptide/protein networks based on the (Fisher’s Z transformed) sample correlation matrix (2a). Next, we calculate the fuzzy logic weight matrix as shown in 2b. The quality and quantity criterion is implemented and $K=39$ is selected, and the procedure is demonstrated in 2c. The network detection is performed to cut edges, allocate correlated features to each other 2d. Based on the permutation test, 8 networks are detected. Furthermore, inside and outside network edges show distinct distributions of Fisher’s Z transformed correlations 2e. We apply the topology/network oriented adaptive decision/thresholding rules to estimate \hat{E} and the covariance/correlation matrix 2f. Note that 2e only identify two components of positively correlated edges and the null, without the negatively correlated edge component. As a result, the negative edges are thresholded. Since the null distribution in 2e seems to be symmetric, based on the Bayes factor decision rule we are confident that edges with high negative correlations are false positive. The network detection results could provide informative inferences about the between feature relationship. In this example data set, each network represents a group of related protein and peptides that could be confirmed by proteomics mass spectrometry literature. For example, the most correlated network 4 consists a list of proteins of normal and variant hemoglobins with one and two charges (Lee *et al*, 2011) including normal hemoglobins α and β with one charge and two charges (at m/z 15127, 15868, 7564, and 7934). The highly correlated networks of biomedical features could potentially provide a set of biomarkers for future research that allow to borrow power between each other.

6 Discussion and Conclusion

The large covariance/correlation matrix of data sets from high-throughput biomedical assays often demonstrate complex, yet highly organized, topology of the underlying physiological and biological machinery. There have been unmet needs of statistical methodologies to simultaneously estimate the covariance matrix and reveal the underlying topological structure. The regularization methods

(e.g. shrinkage or thresholding) are exploited to estimate the covariance matrix. On the hand, the community detection algorithms (e.g. profile likelihood and modularity maximization based on SBM) are employed to explore the graph topological structures, and the results heavily depend on two factors: the similarity metrics and number of clusters. We develop a novel strategy to bridge the covariance estimation and graph topological structure for network induced covariance matrix estimation.

The NICE framework at least makes three novel contributions. First, the fuzzy logic metric provides a sensitive and robust scale to detect the networks because the accuracy of clustering findings primarily depends the similarity metrics. Second, the quality and quantity criterion is a efficient and data-driven heuristic not only to objectively select optimal tuning parameter (i.e. K), but also to guide regularization with graph topology oriented adaptive thresholding stringent levels. A larger C will cut more edges and keep less edges within the networks, and the edges outside and inside of the networks are subject to more stringent thresholding levels because 1) the number of inside of edges are less; and 2) the mean of two distributions are more separate (see [2e](#)). Note that different from all community detection algorithms, our selected tuning parameter C (by the quantity and quality criterion) does not determine the final number of detected networks and a network must pass the permutation test significance level. For example, our example set has $K=39$ but only 8 networks are detected. Therefore, the quality and quantity criterion is a new regularization computational strategy which is distinct from the lasso type ℓ_1 and ℓ_2 shrinkage (e.g. glasso) and adaptive thresholding algorithms because it implement the regularization based on the topology structure constraint and select optimal tuning parameter objectively (less ad-hoc). Last, our covariance matrix estimation (thresholding strategy) could reduce both false positive and false negative discovery rate by leveraging the graph topological structures. The adaptive thresholding rules depends on the inherent topology of G , for example, if the graph is totally random our strategy would be similar to hard thresholding ([Bickel and Levina, 08](#)). In this case, the univariate correlation thresholding method seems to provide satisfactory performance ([Friedman *et al*, 2010](#)). In our applications, only positive (correlation) edges are organized in graph topology and the negative (correlation) edges are randomly distributed. Based on the Bayes factor decision rule, none of

negative (correlation) edges are suprathreshold. In the future, we will examine whether the graph topology structures could include organized negative (correlation) edges, and negative (correlation) edges and positive (correlation) edges could jointly comprise organized topology structures.

The simulation studies and example data set application have demonstrated excellent performance of the NICE algorithm. The computational cost of NICE algorithm is low (for our simulation example the algorithm only takes 40 seconds using i7 CPU and 24G memory), and thus it is ready to scale up for larger data sets. In addition, the NICE algorithm is not restricted for multivariate Gaussian distributed data and it is straightforward to extend the sample correlation matrix to other sample metrics, for example maximal information coefficients ([Kinney and Atwal, 2014](#)) for continuous data and polychoric correlation coefficient for categorical data ([Bonett and Price, 2005](#)) because both fuzzy logic metric and graph topology oriented thresholding are based on the empirical distribution of the coefficients.

Acknowledgements

The research is based upon work supported by the Office of the Director of National Intelligence (ODNI), Intelligence Advanced Research Projects Activity (IARPA), via DJF-15-1200-K-0001725.

Appendix

Proof of Lemma 3.2

Proof. For any i, j , let $Y_k = X_{i,k}X_{j,k}$. Then Y_1, \dots, Y_n are independent and identically distributed. By Condition 3.1, $\Pr[|Y_k| < M^2] = 1$. Define

$$z_{i,j}^{(n)} = g(Y_1, \dots, Y_l, \dots, Y_n) = \frac{1}{2} \log \left(\frac{1 + \sum_{k \neq l}^n Y_k/n + Y_l/n}{1 - \sum_{k \neq l}^n Y_k/n - Y_l/n} \right).$$

Then for all $l = 1, \dots, n$, by Taylor expansion, we have

$$\begin{aligned} & g(Y_1, \dots, Y_l, \dots, Y_n) - g(Y_1, \dots, Y'_l, \dots, Y_n) \\ &= \sum_{k=1}^{\infty} \frac{\partial^k g}{\partial Y_l^k}(Y_1, \dots, Y'_l, \dots, Y_n) \frac{(Y_l - Y'_l)^k}{k!} \end{aligned}$$

where

$$\frac{\partial^k g}{\partial Y_l^k}(Y_1, \dots, Y'_l, \dots, Y_n) = \frac{(k-1)!}{2n^k} \left(\frac{(-1)^{k+1}}{(1 + \hat{\rho}_{i,j}^{(n)})^k} + \frac{1}{(1 - \hat{\rho}_{i,j}^{(n)})^k} \right),$$

By Condition 3.1, $|\rho_{i,j}| < 1$ and strong law of large number, $\hat{\rho}_{i,j}^{(n)} < 1$ with probability one. Thus, there exists $N > 0$ and $K_0 > 0$, for all $n > N$, we have

$$\sup_{Y_1, \dots, Y_n, Y'_l} |g(Y_1, \dots, Y_l, \dots, Y_n) - g(Y_1, \dots, Y'_l, \dots, Y_n)| \leq \frac{K_0}{n}$$

By the McDiarmid inequality, for all $n \geq N$, we have

$$\Pr[|z_{i,j}^{(n)} - \mathbb{E}[z_{i,j}^{(n)}]| > \epsilon] \leq \exp\left(-\frac{2n\epsilon^2}{K_0^2}\right).$$

Thus,

$$\Pr[\sqrt{n}|z_{i,j}^{(n)} - \mathbb{E}[z_{i,j}^{(n)}]| > \epsilon] \leq \exp\left(-\frac{2}{K_0^2}\epsilon^2\right).$$

Taking $K = 2/K_0^2 > 0$ completes the proof. □

Proof of Lemma 3.4

Proof. When $e_{i,j} = 1$ and $\mu_{i,j} > 0$, then

$$\begin{aligned}
& \Pr \left[\frac{\sum_{i',j'} e_{i',j'} \phi\{\sqrt{n}(z_{i,j}^{(n)} - \mu_{i',j'})\}}{\{p_n(p_n - 1)/2 - q_n\} \phi(\sqrt{n}z_{i,j}^{(n)})} \leq T \right] \\
& \leq \Pr \left[\frac{\phi\{\sqrt{n}(z_{i,j}^{(n)} - \mu_{i,j})\}}{\{p_n(p_n - 1)/2 - q_n\} \phi(\sqrt{n}z_{i,j}^{(n)})} \leq T \right] \\
& = \Pr \left[-(z_{i,j}^{(n)} - \mu_{i,j})^2 + z_{i,j}^{2(n)} \leq \frac{2}{n} [\log(T) + \log\{p_n(p_n - 1)/2 - q_n\}] \right] \\
& = \Pr \left[z_{i,j}^{(n)} \leq \frac{1}{2}\mu_{i,j} + \frac{1}{\mu_{i,j}n} [\log(T) + \log\{p_n(p_n - 1)/2 - q_n\}] \right] \\
& = \Pr \left[\sqrt{n}(z_{i,j}^{(n)} - \mu_{i,j}) \leq -\sqrt{n}\mu_{i,j}/2 + \frac{1}{\mu_{i,j}\sqrt{n}} \{\log(T) + \log\{p_n(p_n - 1)/2 - q_n\}\} \right] \\
& \leq \Pr \left[\sqrt{n}(z_{i,j}^{(n)} - \mu_{i,j}) \leq -\sqrt{n}\mu_{\inf}/2 + \frac{1}{\mu_{\sup}\sqrt{n}} \{\log(T) + \log(\{p_n(p_n - 1)/2 - q_n\})\} \right],
\end{aligned}$$

where $\mu_{\sup} = \sup_{i,j} \{|\mu_{i,j}| : e_{i,j} = 1\}$ and μ_{\inf} is defined in Condition 3.2. Note that $E[z_{i,j}^{(n)}] = \mu_{i,j} + o(n^{-1/2})$. There exists N_2 , for all $n > N_2$, such that $\sqrt{n}(\mu_{i,j} - E[z_{i,j}^{(n)}]) < 1$. Then $-\sqrt{n}E[z_{i,j}^{(n)}] - 1 < -\sqrt{n}\mu_{i,j}$ and thus,

$$\begin{aligned}
& \Pr \left[\sqrt{n}(z_{i,j}^{(n)} - \mu_{i,j}) \leq -\sqrt{n}\mu_{\inf}/2 + \frac{1}{\mu_{\sup}\sqrt{n}} \{\log(T) + \log(p_n(p_n - 1)/2 - q_n)\} \right] \\
& \leq \Pr \left[\sqrt{n}(z_{i,j}^{(n)} - E[z_{i,j}^{(n)}]) \leq -\sqrt{n}\mu_{\inf}/2 + \frac{1}{\mu_{\sup}\sqrt{n}} \{\log(T) + \log(p_n(p_n - 1)/2 - q_n)\} + 1 \right]
\end{aligned}$$

By Condition 3.2, we have $\mu_{\inf} = c_0 n^{-1/2+\tau}$ with $\tau > 0$, then $\mu_{\sup} > c_0 n^{-1/2+\tau}$ and . Also, by Conditions 3.3 and 3.4, we have $\log\{p_n(p_n - 1)/2 - q_n\} = o(n^{2\tau})$, then there exists N_1 such that for all $n > N_1$ we have $n^{-\tau} \log\{T(p_n(p_n - 1)/2 - q_n)\} < c_0^2 n^\tau / 8$ and $n^\tau > 8/c_0$. By Lemma 3.2,

$$\begin{aligned}
& \Pr \left[\frac{\sum_{i',j'} e_{i',j'} \phi\{\sqrt{n}(z_{i,j}^{(n)} - \mu_{i',j'})\}}{\{p_n(p_n - 1)/2 - q_n\} \phi(\sqrt{n}z_{i,j}^{(n)})} \leq T \right] \\
& \leq \Pr \left[\sqrt{n}(z_{i,j}^{(n)} - \mu_{i,j}) \leq -\frac{c_0}{4} n^\tau \right] \leq \exp \left(-\frac{c_0^2 K n^{2\tau}}{16} \right).
\end{aligned}$$

When $\mu_{i,j} < 0$, based on similar arguments, we have

$$\begin{aligned} & \Pr \left[\frac{\sum_{i',j'} e_{i',j'} \phi\{\sqrt{n}(z_{i,j}^{(n)} - \mu_{i',j'})\}}{\{p_n(p_n - 1)/2 - q_n\} \phi(\sqrt{n}z_{i,j}^{(n)})} \leq T \right] \\ & \leq \Pr \left[-\sqrt{n}(z_{i,j}^{(n)} - \mu_{i,j}) \leq -\frac{c_0}{4}n^\tau \right] \leq \exp \left(-\frac{c_0^2 K n^{2\tau}}{16} \right). \end{aligned}$$

Taking $C_1 = c_0^2 K/16$ completes the proof for the case when $e_{i,j} = 1$.

When $e_{i,j} = 0$, then

$$\begin{aligned} & \Pr \left[\frac{\sum_{i',j'} e_{i',j'} \phi\{\sqrt{n}(z_{i,j}^{(n)} - \mu_{i',j'})\}}{(p_n(p_n - 1)/2 - q_n) \phi(\sqrt{n}z_{i,j}^{(n)})} > T \right] \\ & \leq \Pr \left[\frac{q_n \phi\{\sqrt{n}(z_{i,j}^{(n)} - \mu_{\inf}/3)\}}{(p_n(p_n - 1)/2 - q_n) \phi(\sqrt{n}z_{i,j}^{(n)})} > T, |z_{i,j}^{(n)}| \leq \mu_{\inf}/3 \right] \\ & \quad + \Pr \left[\frac{\sum_{i',j'} e_{i',j'} \phi\{\sqrt{n}(z_{i,j}^{(n)} - \mu_{i',j'})\}}{(p_n(p_n - 1)/2 - q_n) \phi(\sqrt{n}z_{i,j}^{(n)})} > T, |z_{i,j}^{(n)}| > \mu_{\inf}/3 \right] \\ & \leq \Pr \left[\sqrt{n}z_{i,j}^{(n)} > \sqrt{n}(\mu_{\inf}/6) + \frac{3}{\mu_{\inf}\sqrt{n}} \log \left(T \times \frac{p_n(p_n - 1)/2 - q_n}{q_n} \right) - 1 \right] + \Pr \left[|z_{i,j}^{(n)}| > \mu_{\inf}/3 \right]. \end{aligned}$$

By Condition 3.4, $\lim_{n \rightarrow \infty} \log\{(p_n(p_n - 1)/2 - q_n)/q_n\} = \pi_0/(1 - \pi_0)$, there exists N_0 such that for all $n > N_0$, $\log\{T(p_n(p_n - 1)/2 - q_n)/q_n\} > 0$ and $n^\tau > 12/c_0$. Thus,

$$\begin{aligned} & \Pr \left[\frac{\sum_{i',j'} e_{i',j'} \phi\{\sqrt{n}(z_{i,j}^{(n)} - \mu_{i',j'})\}}{(p_n(p_n - 1)/2 - q_n) \phi(\sqrt{n}z_{i,j}^{(n)})} > T \right] \\ & \leq \Pr \left[\sqrt{n}z_{i,j}^{(n)} > c_0 n^\tau / 12 \right] + \Pr \left[\sqrt{n}|z_{i,j}^{(n)}| > c_0 n^\tau / 3 \right] \leq 3 \exp \left(-\frac{c_0^2 K}{144} n^{2\tau} \right). \end{aligned}$$

Taking $C_0 = c_0^2 K/144$, $C_2 = 3$ and $N_T = \max\{N_0, N_1, N_2\}$ completes the proof for all the cases. \square

Proof Lemma 3.5

Proof. Since $T > (1 - \pi_0)/\pi_0$. Then there exists $\epsilon > 0$ such that $T - \epsilon > (1 - \pi_0)/\pi_0$. By Lemma 3.3 and Condition 3.4, there exists $N_1 > 0$, for all $n > N_1$ such that

$$\frac{\pi_1^{(n)} f_1^{(n)}(z_{i,j}^{(n)})}{\pi_0^{(n)} f_0^{(n)}(z_{i,j}^{(n)})} > \frac{\sum_{i',j'} e_{i',j'} \phi\{\sqrt{n}(z_{i,j}^{(n)} - \mu_{i',j'})\}}{(p_n(p_n - 1)/2 - q_n)\phi(\sqrt{n}z_{i,j}^{(n)})} - \epsilon,$$

$$\frac{\pi_1^{(n)} f_1^{(n)}(z_{i,j}^{(n)})}{\pi_0^{(n)} f_0^{(n)}(z_{i,j}^{(n)})} < \frac{\sum_{i',j'} e_{i',j'} \phi\{\sqrt{n}(z_{i,j}^{(n)} - \mu_{i',j'})\}}{(p_n(p_n - 1)/2 - q_n)\phi(\sqrt{n}z_{i,j}^{(n)})} + \epsilon.$$

Then by Lemma 3.4, when $e_{i,j} = 1$,

$$\begin{aligned} \Pr[e_{i,j}^{(n)}(T) = 0] &= \Pr\left[\frac{\pi_1^{(n)} f_1^{(n)}(z_{i,j}^{(n)})}{\pi_0^{(n)} f_0^{(n)}(z_{i,j}^{(n)})} \leq T\right] \\ &\leq \Pr\left[\frac{\sum_{i',j'} e_{i',j'} \phi\{\sqrt{n}(z_{i,j}^{(n)} - \mu_{i',j'})\}}{(p_n(p_n - 1)/2 - q_n)\phi(\sqrt{n}z_{i,j}^{(n)})} \leq T + \epsilon\right] \leq \exp(-C_1 n^{2\tau}). \end{aligned}$$

when $e_{i,j} = 0$,

$$\begin{aligned} \Pr[e_{i,j}^{(n)}(T) = 1] &= \Pr\left[\frac{\pi_1^{(n)} f_1^{(n)}(z_{i,j}^{(n)})}{\pi_0^{(n)} f_0^{(n)}(z_{i,j}^{(n)})} > T\right] \\ &\leq \Pr\left[\frac{\sum_{i',j'} e_{i',j'} \phi\{\sqrt{n}(z_{i,j}^{(n)} - \mu_{i',j'})\}}{(p_n(p_n - 1)/2 - q_n)\phi(\sqrt{n}z_{i,j}^{(n)})} > T - \epsilon\right] \leq C_2 \exp(-C_0 n^{2\tau}). \end{aligned}$$

Taking $C_3 = \max\{1, C_2\}$ and $C_4 = \min\{C_0, C_1\}$, thus,

$$\Pr[e_{i,j}^{(n)}(T) \neq e_{i,j}] \leq C_3 \exp(-C_4 n^{2\tau}).$$

□

Proof of Lemma 3.6

Proof. Since $T > (1 - \pi_0)/\pi_0$, then there exists $\epsilon > 0$ such that $T - \epsilon > (1 - \pi_0)/\pi_0$. By Condition 3.5, there exists $N_0 > 0$, for all $n > N_0$ and all i, j such that

$$\frac{\widehat{\pi}_1^{(n)} \widehat{f}_1^{(n)}(z_{i,j}^{(n)})}{\widehat{\pi}_0^{(n)} \widehat{f}_0^{(n)}(z_{i,j}^{(n)})} > \frac{\pi_1^{(n)} f_1^{(n)}(z_{i,j}^{(n)})}{\pi_0^{(n)} f_0^{(n)}(z_{i,j}^{(n)})} - \epsilon, \quad \text{and} \quad \frac{\widehat{\pi}_1^{(n)} \widehat{f}_1^{(n)}(z_{i,j}^{(n)})}{\widehat{\pi}_0^{(n)} \widehat{f}_0^{(n)}(z_{i,j}^{(n)})} < \frac{\pi_1^{(n)} f_1^{(n)}(z_{i,j}^{(n)})}{\pi_0^{(n)} f_0^{(n)}(z_{i,j}^{(n)})} + \epsilon.$$

By Lemma 3.6, When $e_{i,j} = 1$, then $\Pr[\widehat{e}_{i,j}^{(n)}(T) = 0] \leq \Pr[e_{i,j}^{(n)}(T + \epsilon) = 0] \leq C_3 \exp(-C_4 n^{2\tau})$, and when $e_{i,j} = 0$, then $\Pr[\widehat{e}_{i,j}^{(n)}(T) = 1] \leq \Pr[e_{i,j}^{(n)}(T - \epsilon) = 1] \leq C_3 \exp(-C_4 n^{2\tau})$. \square

Proof of Theorem 1

Proof. By Lemma 3.6 and the Bonferroni inequality,

$$\begin{aligned} \Pr\{\widehat{\mathbf{E}}(T) \neq \mathbf{E}\} &= \Pr\left[\bigcup_{i < j} \{\widehat{e}_{i,j}^{(n)}(T) \neq e_{i,j}\}\right] \\ &\leq \sum_{1 \leq i < j \leq p_n} \Pr\left[\widehat{e}_{i,j}^{(n)}(T) \neq e_{i,j}\right] \leq \frac{C_3}{2} p_n(p_n - 1) \exp(-C_4 n^{2\tau}). \end{aligned}$$

By Condition 3.3, $\lim_{n \rightarrow \infty} p_n(p_n - 1) \exp(-C_4 n^{2\tau}) = 0$. This completes the proof. \square

Proof of Theorem 2

Proof. Note that

$$\begin{aligned} &\Pr[\|A(\widehat{\mathbf{R}}; T) - \mathbf{R}\|_\infty > \epsilon] \\ &= \Pr[\|A(\widehat{\mathbf{R}}; T) - \mathbf{R}\|_\infty > \epsilon; \widehat{\mathbf{E}}(T) = \mathbf{E}] + \Pr[\|A(\widehat{\mathbf{R}}; T) - \mathbf{R}\|_\infty > \epsilon; \widehat{\mathbf{E}}(T) \neq \mathbf{E}] \\ &\leq \Pr\left[\max_{i < j, e_{i,j}=1} |\widehat{\rho}_{i,j}^{(n)} - \rho_{i,j}| > \epsilon\right] + \Pr[\widehat{\mathbf{E}}(T) \neq \mathbf{E}] \end{aligned}$$

By Bonferroni inequality and Hoeffding's inequality, we have

$$\Pr \left[\max_{i < j: e_{i,j}=1} |\hat{\rho}_{i,j}^{(n)} - \rho_{i,j}| > \epsilon \right] \leq \sum_{i < j: e_{i,j}=1} \Pr[|\hat{\rho}_{i,j}^{(n)} - \rho_{i,j}| > \epsilon] \leq q_n \exp \left(-\frac{n\epsilon^2}{2M^4} \right).$$

By Conditions 3.3 and 3.4, $q_n = o(n^{2\tau})$. Since $0 < \tau < 1/2$, then $\lim_{n \rightarrow \infty} q_n \exp(-n\epsilon^2/2M^4) = 0$.

By Theorem 1, we have $\lim_{n \rightarrow \infty} \Pr[\hat{\mathbf{E}}(T) \neq \mathbf{E}] = 0$. This completes the proof.

□

False Positive and Negative

We further calculate the expected number of false positive (FP) edges using universal threshold and in/out -community. We denote m as the number of edges $|E|$ and ω as the proportion of edges in the detected communities of SBM.

Applying the universal decision rule with z_0 as threshold:

$$E(\#FP) = m \int_{z_0}^{\infty} \frac{f_0(z)}{\pi_0 f(z)} f(z) dz = m\pi_0 F_0(z_0) = m\omega\pi_0^{in} F_0(z_0) + m(1-\omega)\pi_0^{out} F_0(z_0) \quad (8)$$

where we denote $\int_{z_0}^{\infty} f = F(z_0)$.

For edges in communities:

$$E^{in}(\#FP) = \omega m \int_{z_{in}}^{\infty} \frac{\pi_0^{in} f_0^{in}(z)}{f^{in}(z)} f^{in}(z) dz = \omega m \pi_0^{in} F_0^{in}(z_{in}) \quad (9)$$

For edges outside communities:

$$E^{out}(\#FP) = (1-\omega)m \int_{z_{out}}^{\infty} \frac{\pi_0^{out} f_0^{out}(z)}{f^{out}(z)} f^{out}(z) dz = (1-\omega)m\pi_0^{out} F_0^{out}(z_{out}) \quad (10)$$

where $z_{in} < z_0 < z_{out}$, and $F_0^{out}(z) = F_0^{in}(z) = F_0(z)$. There we expect $E(\#FP) > E^{in}(\#FP) + E^{out}(\#FP)$.

$E^{out}(\#FP)$ (9 + 10) if

$$\begin{aligned} & -\omega m \pi_0^{in} (F_0(z_{in}) - F_0(z_0)) + (1 - \omega) m \pi_0^{out} (F_0(z_0) - F_0(z_{out})) > 0, \\ \Leftrightarrow & \frac{F_0(z_0) - F_0(z_{out})}{F_0(z_{in}) - F_0(z_0)} > \frac{\omega \pi_0^{in}}{(1 - \omega) \pi_0^{out}} \end{aligned} \quad (11)$$

Condition 11 is generally true, and we have run numerous empirical experiments and the results further verify the statement when the network detection results are satisfactory.

On the other hand, we further calculate the expected number of true positive (TP) edges using universal threshold and in/out communities to evaluate the power of our graph topology oriented adaptive thresholding.

Applying the universal decision rule with z_0 as threshold:

$$E(\#TP) = m \int_{z_0}^{\infty} \frac{f_1(z)}{\pi_1 f(z)} f(z) dz = m \pi_1 F_0(z_0) = m \omega \pi_1^{in} F_1(z_0) + m(1 - \omega) \pi_1^{out} F_1(z_0) \quad (12)$$

For edges in communities:

$$E^{in}(\# TP) = \omega m \int_{z_{in}}^{\infty} \frac{\pi_1^{in} f_1^{in}(z)}{f^{in}(z)} f^{in}(z) dz = \omega m \pi_1^{in} F_1^{in}(z_{in}) \quad (13)$$

For edges outside communities:

$$E^{out}(\# TP) = (1 - \omega) m \int_{z_{out}}^{\infty} \frac{\pi_1^{out} f_1^{out}(z)}{f^{out}(z)} f^{out}(z) dz = (1 - \omega) m \pi_1^{out} F_1^{out}(z_{out}) \quad (14)$$

where $z_{in} < z_1 < z_{out}$, and $F_1^{out}(z) = F_1^{in}(z) = F_1(z)$. There we expect $E(\#TP)$ (12) < $E^{in}(\#TP) + E^{out}(\#TP)$ (13 + 14) if

$$\begin{aligned}
& -\omega m\pi_0^{in}(F_1(z_{in}) - F_1(z_0)) + (1 - \omega)m\pi_1^{out}(F_1(z_0) - F_1(z_{out})) < 0, \\
& \Leftrightarrow \frac{F_1(z_0) - F_1(z_{out})}{F_1(z_{in}) - F_1(z_0)} < \frac{\omega\pi_1^{in}}{(1 - \omega)\pi_1^{out}}
\end{aligned} \tag{15}$$

Condition 15 is also generally true, and we have run numerous empirical experiments and the results further verify the statement when the network detection results are satisfactory. Also, when our ‘quality and quantity’ criteria is optimal that all truly connected edges are included in the detected networks and all networks exclusively include truly connected edges, the our adaptive thresholding method ensures perfect detection of truly connected edges with zero false positive discovery. If the assumption of network induced covariance is true, the C selection procedure chooses the parameter to optimize the ‘quality and quantity’ criteria that allows to reduce false positive findings and improve power simultaneously.

Thresholding values

We calculate the thresholding values for edges inside-networks and outside-networks separately, and the cut-off can be linked to the overall local fdr value. Therefore, the computation is more straightforward by using the following cut-offs.

For edges inside networks we would use local fdr cut-off as 0.2,

$$\begin{aligned}
& \frac{\pi_1^{in}f_1(z)}{\pi_0^{in}f_0(z)} = 1 - fdr^{in}/fdr^{in} = 4 \\
& \Leftrightarrow \frac{f_1(z)}{f_0(z)} = 4\frac{\pi_0^{in}}{\pi_1^{in}}
\end{aligned} \tag{16}$$

and if $\frac{f_1(z)}{f_0(z)} > 4\frac{\pi_0^{in}}{\pi_1^{in}}$ we consider the edge is truly connected.

The above cut-off is equivalent to the cut-off for all edges inside and outside the networks by

applying the decision rule of $\frac{f_1(z)}{f_0(z)} > 4 \frac{\pi_0^{in}}{\pi_1^{in}}$:

$$\begin{aligned}
\frac{\pi_1^{all} f_1(z)}{\pi_0^{all} f_1(z)} &= 1 - fdr^{all} / fdr^{all} \\
\Leftrightarrow \frac{f_1(z)}{f_0(z)} \frac{\pi_1^{all}}{\pi_0^{all}} &= 4 \frac{\pi_0^{in}}{\pi_1^{in}} \frac{\pi_1^{all}}{\pi_0^{all}} = 1 - fdr^{all} / fdr^{all} \\
\Leftrightarrow fdr^{all}(in) &= \frac{1}{4 \frac{\pi_0^{in}}{\pi_1^{in}} \frac{\pi_1^{all}}{\pi_0^{all}} + 1}
\end{aligned} \tag{17}$$

For example, if $\pi_0^{in}/\pi_1^{in} = 10$ and $\pi_1^{all}/\pi_0^{all} = 10$, then $fdr^{all}(in)=0.96$ and most edges are not thresholded as the cut-off is loose.

Similarly, for edges outside networks

$$fdr^{all}(out) = \frac{1}{4 \frac{\pi_0^{out}}{\pi_1^{out}} \frac{\pi_1^{all}}{\pi_0^{all}} + 1}$$

if $\pi_0^{out}/\pi_1^{out} = 40$ and $\pi_1^{all}/\pi_0^{all} = 10$, then $fdr^{all}(out)=0.06$ and most edges outside the network are thresholded using a more stringent cut-off.

When the data shows no network structure, for instance, $\pi_0^{in}/\pi_1^{in} = \pi_0^{out}/\pi_1^{out} = 10$ and $\pi_1^{all}/\pi_0^{all} = 10$, then $fdr^{all}(in) = fdr^{all}(out) = 0.2$. Our adaptive thresholding rule boils down to the universal thresholding rule.

References

- Banerjee, O., El Ghaoui, L. and d'Aspremont, A. (2008). Model selection through sparse maximum likelihood estimation for multivariate Gaussian or binary data. *The Journal of Machine Learning Research* **9**, 485-516.
- Besag, J., Kooperberg, C. (1995). On conditional and intrinsic autoregressions. *Biometrika*, **82**(4), 733-746.
- Bickel, P.J., Levina, E. (2008). Covariance regularization by thresholding. *Ann. Statist.* **36**, no. 6,

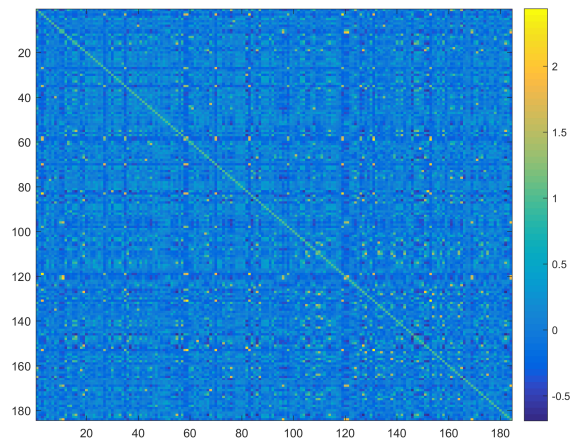
2577–2604.

- Bickel, P. J., Chen, A. (2009). A nonparametric view of network models and NewmanGirvan and other modularities. *Proceedings of the National Academy of Sciences*, **106**(50), 21068-21073.
- Bonett, D. G., Price R. M. (2005). Inferential Methods for the Tetrachoric Correlation Coefficient. *Journal of Educational and Behavioral Statistics*, **30**, 213.
- Cai, T., Liu, W. and Luo, X. (2011). A constrained ℓ_1 minimization approach to sparse precision matrix estimation. *Journal of the American Statistical Association*, **106**, 594–607.
- Cai, T., Liu, W. (2011). Adaptive thresholding for sparse covariance matrix estimation. *J. Amer. Statist. Assoc.* **106** (494), 672–684.
- Cai, T. T., Ren, Z., Zhou, H. H. (2014). Estimating structured high-dimensional covariance and precision matrices: Optimal rates and adaptive estimation. *The Annals of Statistics*, **38**, 2118–2144.
- Chen, S., Li, M., Hong, D., Billheimer, D., Li, H., Xu, B. J., Shyr, Y. (2009). A novel comprehensive wave-form MS data processing method. *Bioinformatics*, **25**(6), 808-814.
- Chen, S., Kang, J., Wang, G. (2015). An empirical Bayes normalization method for connectivity metrics in resting state fMRI. *Frontiers in neuroscience*, **9**, 316-323.
- Chen, S., Kang, J., Xing, Y., Wang, G. (2015). A parsimonious statistical method to detect group-wise differentially expressed functional connectivity networks. *Human brain mapping*, **36**(12), 5196-5206.
- Choi, D. S., Wolfe, P. J., Airolidi, E. M. (2012). Stochastic blockmodels with a growing number of classes. *Biometrika*, **99**, 273-284.
- Chung, F. R. (1997). Spectral Graph Theory (CBMS Regional Conference Series in Mathematics, No. 92), American Mathematical Society.
- Cui, Y., Leng, C., Sun, D. (2016). Sparse estimation of high-dimensional correlation matrices. *Computational Statistics & Data Analysis*, **93**, 390-403.

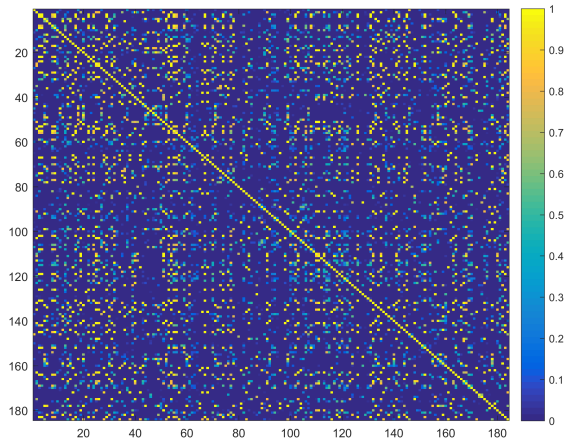
- Donoho, D. L., Johnstone, I. M., Kerkycharian, G. and Picard, D. (1995). Wavelet shrinkage: asymptopia? (with discussion). *Journal of the Royal Statistical Society, Series B* **57**, 301-369.
- Efron, B. (2004). Large-Scale Simultaneous Hypothesis Testing: The Choice of a Null Hypothesis. *Journal of the American Statistical Association*, **99**, 96-104.
- Efron, B. (2007). Size, power and false discovery rates. *The Annals of Statistics*, **35**(4), 1351-1377.
- Efron, B., Turnbull, B., Narasimhan, B. (2008). locfdr: Computes local false discovery rates. *R package*, 195.
- El Karoui, N. (2010). High-dimensionality effects in the markowitz problem and other quadratic programs with linear constraints: risk underestimation. *The Annals of Statistics*, **38**, 3487-3566.
- Fan, J., Liao, Y., Mincheva, M. (2013). Large covariance estimation by thresholding principal orthogonal complements. With 33 discussions by 57 authors and a reply by Fan, Liao and Mincheva. *J. R. Stat. Soc. Ser. B. Stat. Methodol.* **75**, no. 4, 603-680.
- Fan, J., Liao, Y., Liu, H. (2015). Estimating Large Covariance and Precision Matrices. arXiv preprint arXiv:1504.02995.
- Friedman, J., Hastie, T., Tibshirani, R. Sparse inverse covariance estimation with the graphical lasso. (2008). *Biostat.* **9**(3), 432-441.
- Friedman, J., Hastie, T., Tibshirani, R. (2010). Applications of the lasso and grouped lasso to the estimation of sparse graphical models (pp. 1-22). Technical report, Stanford University.
- Lam, C. and Fan, J. (2009). Sparsistency and rates of convergence in large covariance matrix estimation. *Annals of statistics* **37** 42-54.
- Lee, B. S., Jayathilaka, G. L. P., Huang, J. S., Vida, L. N., Honig, G. R., Gupta, S. (2011). Analyses of in vitro nonenzymatic glycation of normal and variant hemoglobins by MALDI-TOF mass spectrometry. *Journal of biomolecular techniques: JBT*, **22**(3), 90.
- Lei, J., Rinaldo, A. (2014). Consistency of spectral clustering in stochastic block models. *The Annals of Statistics*, **43**(1), 215-237.

- Liu, H., Wang, L. and Zhao, T. (2014). Sparse covariance matrix estimation with eigenvalue constraints. *Journal of Computational and Graphical Statistics*, **23**, 439-459.
- Jeffreys, H. (1961). *Theory of Probability*, 3rd ed. Clarendon Press, Oxford.
- Kass, R. E., Raftery, A. E. (1995). Bayes factors. *Journal of the american statistical association*, **90**(430), 773-795.
- Karrer, B., Newman, M. E. (2011). Stochastic block models and community structure in networks. *Physical Review E*, **83**(1), 016107.
- Kinney, J. B., Atwal, G. S. (2014). Equitability, mutual information, and the maximal information coefficient. *Proceedings of the National Academy of Sciences*, **111**(9), 3354-3359.
- Mazumder, R. and Hastie, T. (2012). Exact covariance thresholding into connected components for large-scale graphical lasso. *The Journal of Machine Learning Research*, **13**(1), 781-794.
- Nadakuditi, R. R., Newman, M. E. (2012). Graph spectra and the detectability of community structure in networks. *Physical review letters*, **108**(18), 188701.
- Rothman, A. J., Levina, E. and Zhu, J. (2009). Generalized thresholding of large covariance matrices. *Journal of the American Statistical Association* **104**, 177-186.
- Qi, H. and Sun, D. (2006). A quadratically convergent newton method for computing the nearest correlation matrix. *SIAM journal on matrix analysis and applications* **28** 360-385.
- Scott, J. G., Berger, J. O. (2006). An exploration of aspects of Bayesian multiple testing. *Journal of Statistical Planning and Inference*, **136**(7), 2144-2162.
- Scott, J. G., Berger, J. O. (2010). Bayes and empirical-Bayes multiplicity adjustment in the variable-selection problem. *The Annals of Statistics*, **38**(5), 2587-2619.
- Schäfer, J., Strimmer, K. (2005). A shrinkage approach to large-scale covariance matrix estimation and implications for functional genomics. *Statistical applications in genetics and molecular biology*, **4**(1).

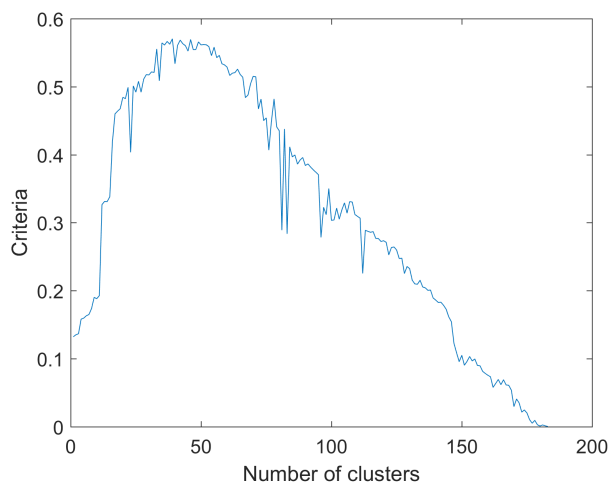
- Shen, X., Pan, W. and Zhu, Y. (2012). Likelihood-based selection and sharp parameter estimation. *Journal of the American Statistical Association* **107** 223232.
- Shi, J., Malik, J. (2000). Normalized cuts and image segmentation. *Pattern Analysis and Machine Intelligence, IEEE Transactions on*, **22**(8), 888-905.
- von Luxburg, U. A tutorial on spectral clustering. (2007), *Stat. Comput.* **17** (4), 395–416.
- Witten, D. M., Friedman, J. H., Simon, N. (2011). New insights and faster computations for the graphical lasso. *Journal of Computational and Graphical Statistics*, **20**(4), 892-900.
- Wu, B., Guan, Z., Zhao, H. (2006). Parametric and nonparametric FDR estimation revisited. *Biometrics*, 62(3), 735-744.
- Yildiz, P. B., Shyr, Y., Rahman, J. S., Wardwell, N. R., Zimmerman, L. J., Shakhtour, B., ... Massion, P. P. (2007). Diagnostic accuracy of MALDI mass spectrometric analysis of unfractionated serum in lung cancer. *Journal of thoracic oncology*, **2**(10), 893-915.
- Yuan, M. and Lin, Y. (2007). Model selection and estimation in the gaussian graphical model. *Biometrika*, **94**, 19–35.
- Yuan, M. (2010). High dimensional inverse covariance matrix estimation via linear programming. *Journal of Machine Learning Research*, **11**, 2261-2286.
- Zhang, C.-H. (2010). Nearly unbiased variable selection under minimax concave penalty. *The Annals of Statistics*, 894942.
- Zhao, Y., Levina, E., Zhu, J. (2011). Community extraction for social networks. *Proceedings of the National Academy of Sciences*, **108**(18), 7321-7326.



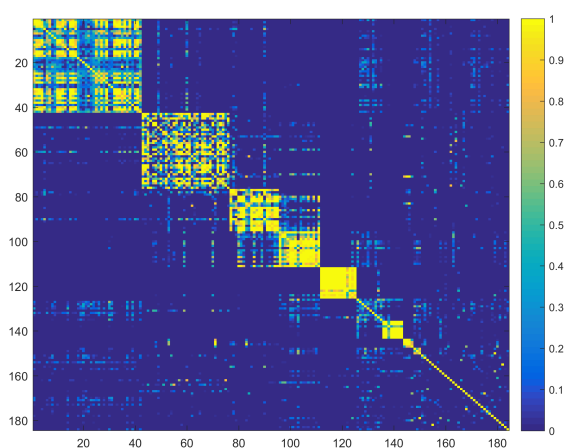
(a) Sample correlation



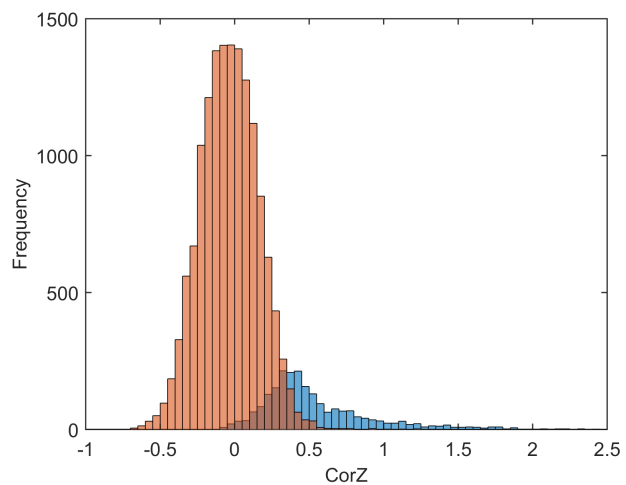
(b) Fuzzy logic weight matrix



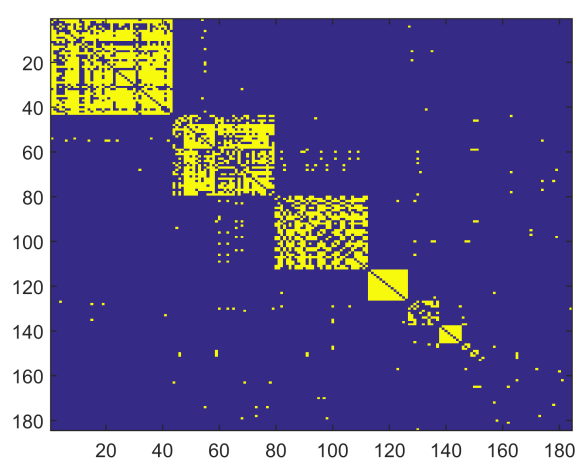
(c) K selection



(d) Network detection: reordered W .



(e) Edges inside and outside networks



(f) Estimated edge set \hat{E}

Figure 2: Application of the NICE to the example data set.